Encapsulation of Aromatic Compounds and a Non-Aromatic Herbicide into a Gadolinium Based Metal-Organic Framework via the Crystalline Sponge Method

Richard D. J. Lunn,[†] Derek A. Tocher,[†] Philip J. Sidebottom,[‡] Mark G. Montgomery,[‡] Adam C. Keates,[‡] Claire J. Carmalt[†]*

[†]UCL Department of Chemistry, 20 Gordon Street, London, WC1H 0AJ

[‡]Syngenta, Jealott's Hill International Research Centre, Bracknell, Berkshire, RG42 6EY

Abstract

The crystalline sponge method (CSM) is a procedure that has the potential to remove the need to have good quality single crystals of the target compound by soaking said compound into a crystalline metal-organic framework (MOF). To increase the range of compounds that can be employed with the CSM a range of different MOFs must be investigated. In this study we have explored the use of a lanthanide-based MOF, RUM-2, recently shown to have potential as a CSM host. Specifically, we have successfully formed five novel inclusion complexes with four aromatic guests 2-phenylethanol, benzyl acetate, benzyl benzoate, vanillin and a non-aromatic herbicide molinate. A detailed analysis of the effect of size on the positions guest molecules sit within the pores of the MOF was performed. The π···π, CH···π, hydrogen bonding and

coordination host-guest and guest-guest interactions utilised in guest ordering were also investigated and the disorder experienced by guest molecules documented.

Introduction

The Crystalline Sponge Method (CSM), first introduced by Fujita *et al.*,[1] describes a procedure designed to circumvent one of the fundamental limitations of single crystal X-ray diffraction (SCXRD), namely the requirement to have good quality single crystals of the target compound. This technique would allow compounds that could not be analysed by SCXRD previously, such as powders, liquids and amorphous solids, to have their chemical structures resolved unambiguously. The procedure outlined seems simple, soak pre-synthesised metal-organic framework (MOF) crystals with a small amount of the target compound for a short period of time. The target compound (referred to as the guest upon encapsulation into the MOF) enters the MOF pores and is ordered via intermolecular interactions between the host MOF and the guest. This allows for the guest to contribute to the diffraction pattern and produce a crystal structure with the guest observed within the host pores after SCXRD analysis.

The CSM has been proven difficult to master,[2] but over the past seven years the usefulness of the technique has been successfully demonstrated. The CSM has been employed to encapsulate many different chemical structures such as drug-like nucleophilic compounds,[3] natural products,[4,5] metabolites,[6,7] ozonides[8] and volatile aromatic isomers such as *cis* and *trans*-asarone.[9] An additional application of the CSM is the structural elucidation of chemical reaction intermediates. If these intermediates are consistent with a speculated reaction mechanism they can aid in their confirmation.[10–13] For example, CSM was used to confirm the syn-addition mechanism for metal-free diboration.[14]

The most commonly used MOF for the CSM is $\{[(ZnI_2)_3(TPT)_2].x(solvent)\}_n$[1,15–19] [**1**; TPT = 2,4,6-tri(4-pyridyl)-1,3,5-trazine]. The TPT linker is highly electron deficient and aromatic allowing for the formation of CH···π and π···π intermolecular interactions between the host

framework and an aromatic guest. Though this MOF has been so widely used it does have some limitations. Firstly, as the pores of **1** are hydrophobic, the MOF is only able to encapsulate hydrophobic compounds. Bringing the MOF into contact with hydrophilic compounds causes the MOF to become damaged and lose its single crystallinity. Secondly, the size of compounds that can be encapsulated is limited by the size of the MOF pores (8 x 5 $Å^2$).[20] Finally the number and type of intermolecular interactions possible is dependent on the MOFs organic linker. Interactions involving **1** are mainly based on its electron deficiency and aromaticity, this can lead to some encapsulated guests exhibiting disorder in their determined structure;[21] therefore it is imperative to research new MOFs to use as crystalline sponges. A series of search parameters has been published previously to aid in the search for appropriate MOFs in crystallographic databases.[20]

To date several different MOFs have been assessed for their ability to act as a crystalline sponge.[22–25] A few MOFs exhibit coordination bonds between the host framework and the guest molecule.[24,25] Coordination of guest molecules can improve the crystallographic model of the guest by increasing guest occupancy and reducing disorder that can be prevalent in MOFs which order guests only *via* CH···π and π···π intermolecular interactions. Recently de Gelder *et al.* demonstrated using a MOF, known as RUM-2 (**2**), as a crystalline sponge by successfully encapsulating a range of simple small molecules such as methanol, pyridine and carvone.[26]

The Gd MOF, **2**, has several features that could be beneficial for use in the CSM. Firstly **2** crystallises in the low symmetry monoclinic space group C2/*c*, which reduces the chance of a guest molecule being located on a symmetry element. Secondly, **2** exhibits channels with dimensions of approximately 11 x 6 $Å^2$ which are slightly larger than the pores of **1**. Therefore, it will be possible to encapsulate larger guests than is possible using **1**. A potential limitation of **2** occurs due to the small width of the MOF channels. Similar to **1**, encapsulation of bulkier target compounds of a three-dimensional nature, will not be possible if they are too large to

enter the MOF channels. Thirdly, de Gelder *et al.*[26] reported that **2** can tolerate a much larger range of solvents than **1**. These range from hydrophobic chloroform and pyridine to hydrophilic solvents such as methanol, dimethylformamide (DMF) and water; which destroy the single crystallinity of **1** due to its hydrophobic nature.[26] The greater stability of **2** can be attributed to the stronger bonds formed between the gadolinium metal atoms and the carboxylate groups of the 1,3,5-benzenetribenzoic acid (H_3BTB) organic linkers. This is in contrast to the weaker bonds formed between the nitrogen lone-pair of TPT and the zinc metal atoms in **1**. The improved stability of **2** will increase the range of guest molecules that it is possible to encapsulate by the CSM.[26] In addition to this the two DMF solvent molecules coordinated to the metal centre in the as-synthesised MOF could be replaced by other guest molecules using coordination bonds which reduces the possibility of guest disorder. It was thus determined that this would be an ideal MOF for further experimentation for use in the CSM.

In this paper we expand on the work described by de Gelder *et al*.[26] and investigate the encapsulation of different guest compounds and how they interact with the host **2**. Herein is described the encapsulation of five new guest compounds into **2** (displayed in Figure 1). Four of the guests were encapsulated using neat liquid guest (2-phenylethanol (**A**), benzyl acetate (**B**), benzyl benzoate (**C**) and molinate (**D**)) and one guest, vanillin (**E**; powder), was encapsulated as a 1 M solution in methanol. These guests were chosen for encapsulation as they are either soluble or miscible with methanol and/or DMF, vary in size and all the guests contain either a primary alcohol, aldehyde, ester or S-thiocarbamate functional group which could allow for guest coordination to the host.

Results

The host MOF crystals were synthesised according to a literature procedure,[26] after which the crystals were stored in methanol at 25 °C until required for guest encapsulation experiments. The removal of the DMF solvent and replacement with methanol was confirmed

through SCXRD analysis.[26] Methanol was chosen as a suitable pore solvent because of the solubility of the guest compounds and methanol is more labile than the DMF molecules that are found in the pores of the as-synthesised **2**. This also reduces the chance of a guest molecule occupying the same site as the solvent molecule which has been found previously to increase the challenge of structure refinement.[26]

Guest encapsulations were performed in a screw capped vials with the crystals submerged in either neat guest or guest solution and the vial stored in an incubator maintained at 25 °C. This minimises any possible temperature fluctuations that may be experienced in a laboratory which could produce defects in the crystals. During the encapsulation procedure the crystals were monitored to ensure the crystal quality was being maintained, if the crystals were damaged it is probable that the crystals had been soaking for too long and therefore the experiment would be repeated for a shorter period of time. After the crystals had soaked in guest for a specific time (supporting information Table S1), a good quality single crystal was chosen for SCXRD analysis.

All five of the inclusion complexes presented here are novel, and all exhibit the same centrosymmetric C2/*c* space group symmetry as seen in the as-synthesised MOF.[26] Each complex shows similar unit cell parameters to the as-synthesised **2**, with the exception of the inclusion complex **2.C** which displays unit cell parameters with shorter *a* and *c* lengths and a smaller β angle than those observed for **2.** The guests were all encapsulated with high occupancies ranging from 50% to 100% (supporting information).

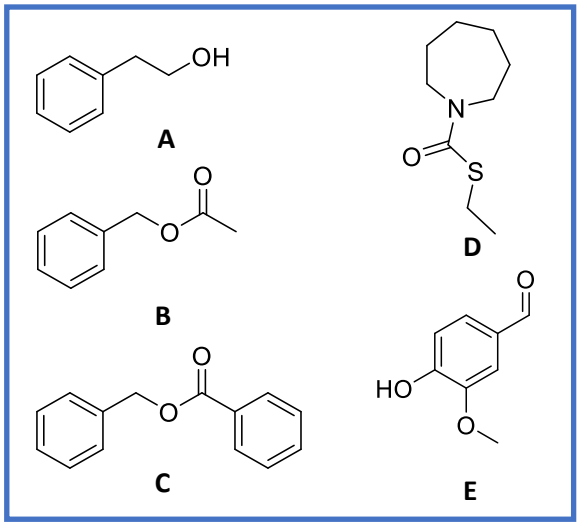

Figure 1. The five guest molecules chosen for encapsulation into **2**. Guests include: 2-phenylethanol (**A**), Benzyl acetate (**B**), Benzyl benzoate (**C**), Molinate (**D**) and Vanillin (**E**).

Effect of Size

First the effect of increasing the size of the guest was investigated, specifically looking at the impact on the positions within the MOF pores that the guests prefer to occupy and what host-guest intermolecular interactions were formed. To investigate this the inclusion complexes formed by the encapsulation of 2-phenylethanol, benzyl acetate and benzyl benzoate were analysed and compared.

As can be observed upon studying the unit cell diagrams (Figure 2) the positions the guests occupy are quite different, though some similarities are present. Inclusion complexes **2.A** and **2.B** both share the positions identified in green and red, in these positions both **A** and **B** coordinate to the host framework with average Gd-O bond lengths of 2.469 Å and 2.489 Å respectively. These lengths are very similar to those found in previously reported inclusion complexes for 1-methyl-2-pyrrlidone (2.430 Å), DMF (2.435 Å) and methanol (2.446 Å) in **2**.[26] Coordination occurs *via* a lone pair of electrons on the oxygen atom of the hydroxyl group

(O7 and O8) in **A** or carbonyl group (O7 and O9) in **B** and the gadolinium metal of the host. The space occupied by molecules shown in green is extremely similar, mainly differing due to the sizes of the molecules. Both guests displayed as green in Figure 2 also show additional CH···π interactions with the host allowing for extra stabilisation with the guests' phenyl rings. Some of the CH···π interactions are comparable; both molecules exhibit CH···π interactions with an opposite carboxylate aromatic ring of the BTB linker with CH···centroid$_{guest}$ distances of 3.769 Å, 3.994 Å and 3.720 Å, 4.149 Å for **A** and **B** respectively. Due to its proximity with the yellow guest molecule, **A** exhibits an additional hydrogen bonding interaction not observed with **B**, and these interactions are shown in Figure 3.

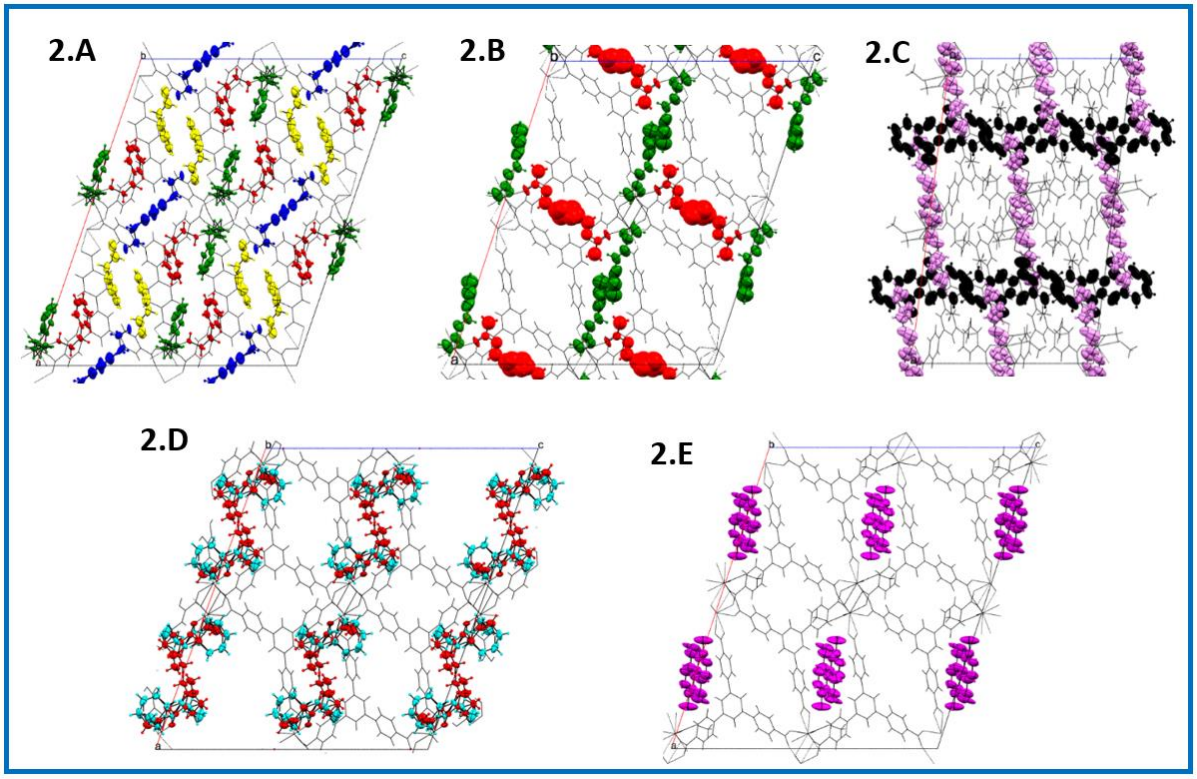

Figure 2. Unit cell diagrams of the inclusion complex crystal structures viewed down the crystallographic *b* axis. (**2.A**) 2-phenylethanol, (**2.B**) Benzyl acetate, (**2.C**) Benzyl benzoate, (**2.D**) Molinate and (**2.E**) Vanillin. Molecules are coloured by their positional equivalence and the host framework is displayed as a wireframe.

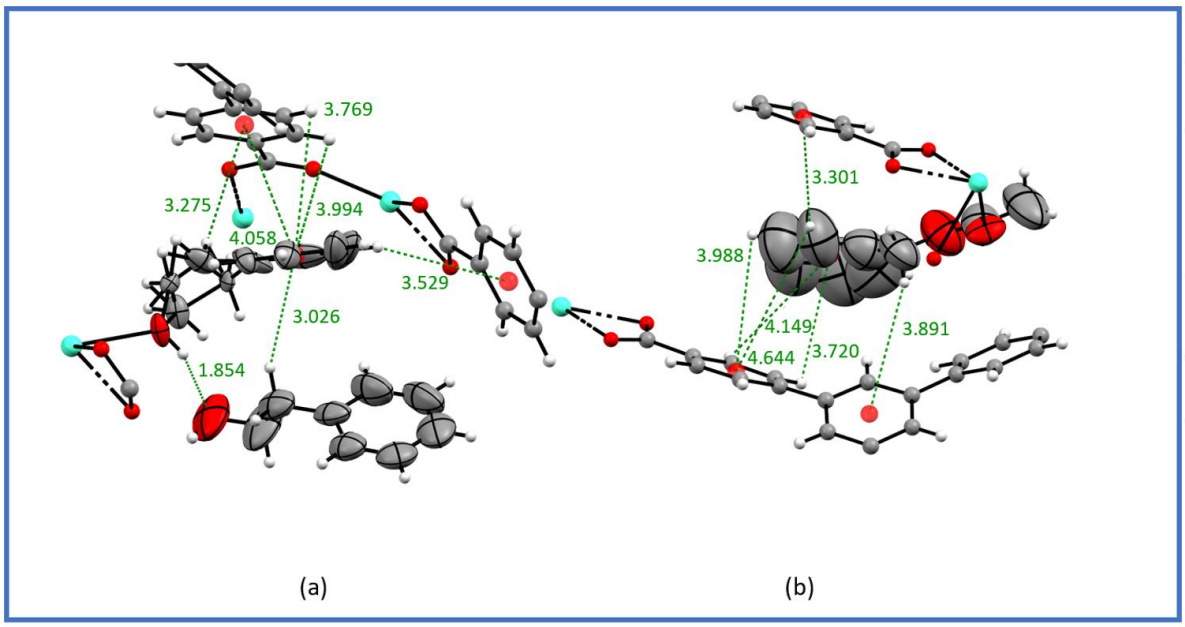

Figure 3. ORTEP diagrams showing guests displayed as ellipsoids at 50% probability and host framework as a ball and stick model. The intermolecular interactions and distances of the green guest molecule (Figure 2) in complex (a) **2.A** and (b) **2.B**. Centroids are displayed as red spheres and interactions are represented as dotted lines. Interaction distances are displayed in angstroms.

The molecules displayed in red (Figure 2) occupy the equivalent coordination site in both inclusion complexes. However, the orientation of each guest is unique. The red molecule in **2.A** is orientated with its molecular axis roughly parallel to the crystallographic *a* axis whereas the **B** molecule is orientated roughly parallel to the crystallographic *c* axis and is disordered over two positions related by two-fold rotational symmetry. Both molecules are also stabilised by extra CH···π and π···π interactions on the aromatic rings. Guest **C** does not coordinate with the host framework and is only ordered by Van der Waals interactions, this is likely due to the larger size of **C**. This was also observed in the publication by de Gelder *et al.*[26] where carvone does not coordinate to the host framework but smaller guests such as methanol, DMF, pyridine and 1-methyl-2-pyrrolidone do coordinate.

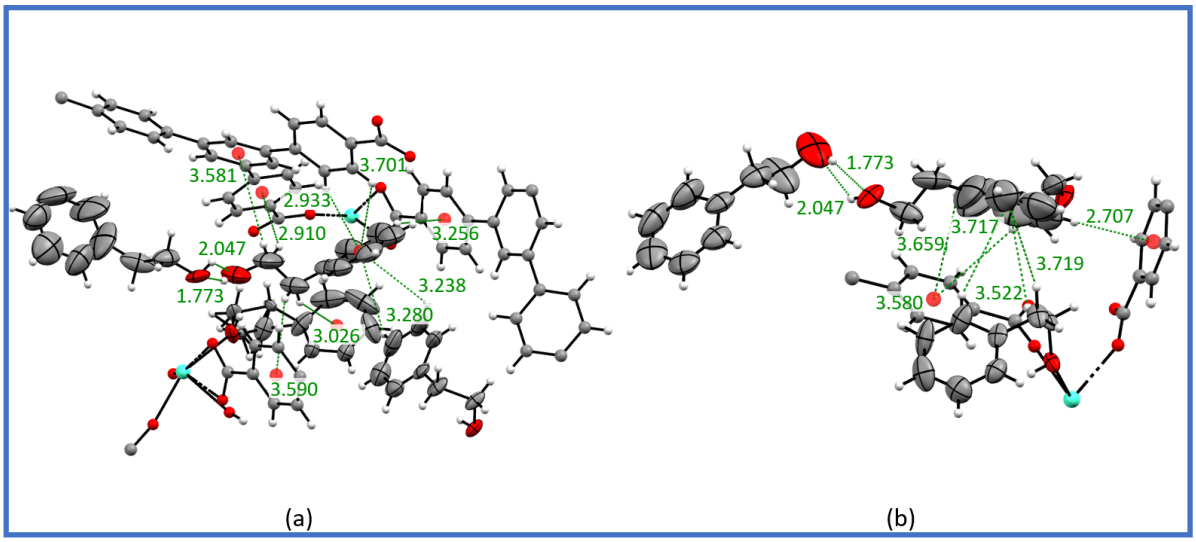

Figure 4. ORTEP diagrams showing guests displayed as ellipsoids at 50% probability and host framework as a ball and stick model. The intermolecular interactions and distances for the **2.A** guest molecule with (a) yellow and (b) blue colouration in Figure 2. Centroids displayed as red spheres; interactions are represented as green dotted lines. Interaction distances are displayed in angstroms.

The inclusion complex **2.A** also has two guest molecules that are ordered solely by Van der Waals interactions (displayed in blue and yellow in Figure 2), neither of these positions are common with those occupied by guests **B** or **C**. The yellow guest molecule in **2.A** is ordered by CH···π interactions with the host and coordinated guest molecules as shown in Figure 4a. The molecule shown in blue occupies a space between four BTB linkers and two red coordinated guest molecules. In this space, **A** forms several unique CH···π interactions with two of the BTB linkers and one of the coordinated guest molecules. Two hydrogen bonds are formed with the molecule with yellow colouration (Figure 4b). As this molecule sits on a two-fold rotational symmetry axis, the unique intermolecular distances between the host and the guest are repeated with the other guest molecule and two BTB linkers. Both the blue and yellow guest molecules share the two unique hydrogen bonding interactions with each other, which help to order the position of the alcohol functional groups in the structure of the guest.

The unit cell parameters for complex **2.C** show a shorter *a* and *c* length and smaller *β* angle than those found for **2.A**, **2.B** and the as-synthesised **2**, which can be seen in Figure 2. Two molecules of **C** were encapsulated into the asymmetric unit of **2.C** where both guest molecules sit on inversion centres, in comparison to four molecules encapsulated into the asymmetric unit of **2.A** where three guest molecules sit in general positions and one sits on a two-fold rotational symmetry axis. The difference in the number of guest molecules encapsulated is clearly due to the increased steric requirements involved when encapsulating **C**. Studying the spacefill unit cell models for both complexes **2.A** and **2.C** (supporting information Figure S2) shows that all the available space is occupied. Two guest molecules were also modelled in complex **2.B,** but studying the spacefill model (see supporting information Figure S2) reveals that there is a large amount of empty space within the unit cell. This can be attributed to either an additional guest molecule or solvent molecules that could not be modelled in the XRD analysis.

The two guest molecules encapsulated into complex **2.C** form many intermolecular interactions with the host framework. The guest molecule displayed in black (Figure 2) forms several unique intermolecular interactions with the host and the other guest molecule consisting of CH···π, π···π and hydrogen bonding interactions. Due to the presence of a centre of inversion in the middle of the guest molecule these same unique interactions were also observed on the symmetry generated aromatic ring (Figure 5a,c). For the guest displayed in violet (Figure 2), the centre of inversion was found in the middle of a phenyl ring, which causes a disordered model of the guest with one benzyl ring in common. This guest molecule forms many unique interactions with the other guest molecule (black in Figure 2) and the host framework as seen in Figure 5b,c.

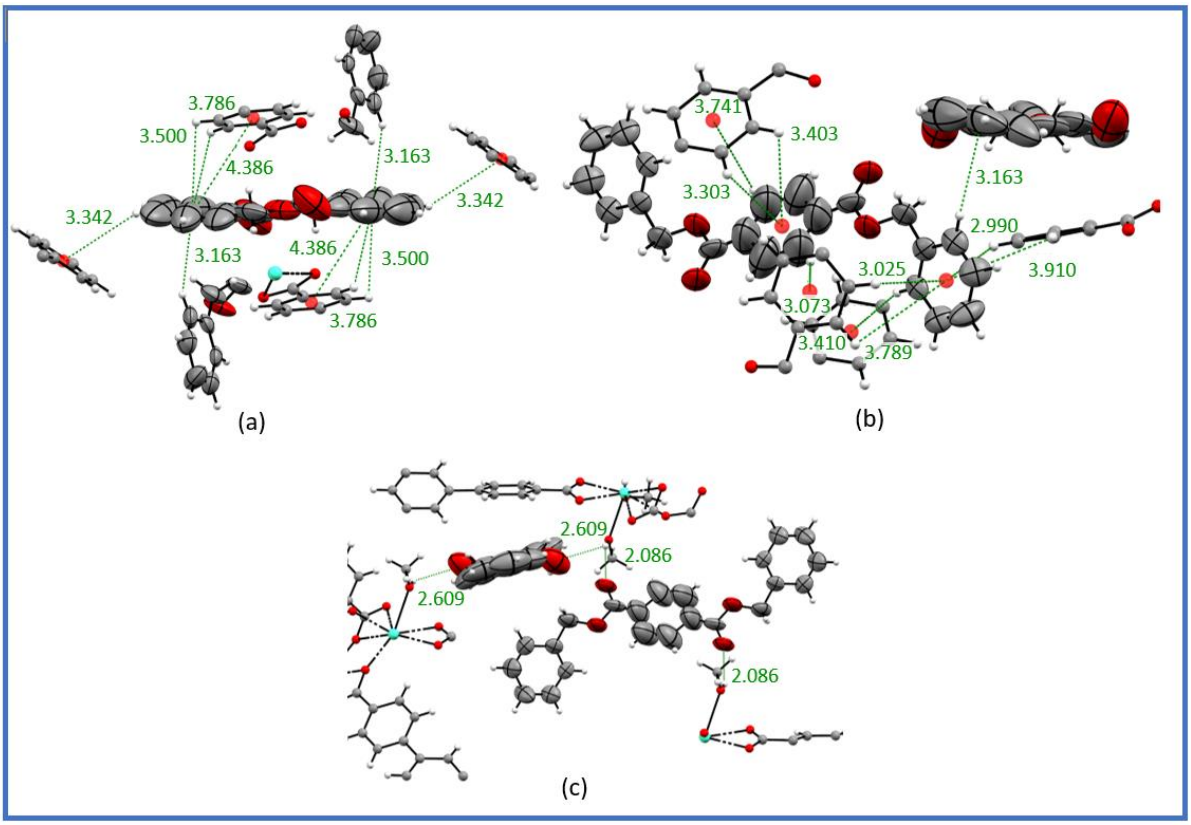

Figure 5. ORTEP diagrams showing guests displayed as ellipsoids at 50% probability and host framework as a ball and stick model. The intermolecular host-guest interactions and distances of: (a) **C** with black colouration in Figure 2, (b) **C** displayed in violet (Figure 2). (c) shows the intermolecular hydrogen bonding interactions. Centroids displayed as red spheres; interactions are represented as green dotted lines. Interaction distances are displayed in angstroms.

Encapsulation of a Herbicide

Molinate, a herbicide used to control the weeds in rice fields,[27] was also encapsulated within the pores of **2** forming complex **2.D**. Molinate is one in a number of herbicides with the thiocarbamate functional group ($RSC(=O)NR_2$).[28] To the best of our knowledge this is the first commercial herbicide active ingredient to be encapsulated into a MOF using the CSM. Unlike the other compounds reported here molinate has no aromatic groups and the only π bonding interactions is the C=O group, therefore molinate is unlikely to form π···π interactions for guest

ordering and has a reduced ability to form CH···π interactions as they can now only form using the π system of the host framework. Consequently, the main interaction expected to be employed for guest ordering would be coordination of the C=O of the thiocarbamate functional group with the MOF metal centre.

This in fact was the case as one disordered guest molecule was successfully located and refined within the asymmetric unit as being coordinated to the Gd metal of the host. Unlike the other guests studied here the disorder experienced by **D** was not due to it sitting on the same site as a symmetry element, therefore the two disordered parts of **D** form different CH···π interactions with the BTB linker of the host framework (Figure 6a,b). Part 1 (displayed in cyan in Figure 2) is orientated such that the seven-membered ring of **D** is only close enough to interact with two terminal phenyl rings of the BTB linker. The C30-S1-C29-C28 torsion angle, as illustrated in Figure 6c,d, are very different in the two disordered components. The torsion angle in part 1 is -78.8° which orientates atom C28 towards the central ring of a BTB linker to facilitate a CH···π interaction. This does not happen in part 2 (displayed in red in Figure 2) in which the C30-S1-C29-C28 torsion angle, is 173.2° making the chain nearly flat. Overall part 1 of **D** only forms five CH···π interactions with the host. Part 2 of the model is in a more favourable position for CH···π interaction forming eight such interactions with the host.

On studying the spacefill unit cell model using mercury[29] (supporting information Figure S2), a large amount of unused space was observed in the unit cell. This space could contain either another guest molecule or additional solvent molecules that were too disordered to be identified and modelled. When examining the position of the MOF pores occupied by **D**, a clear comparison can be made with guests **A** and **B**. **D** shares the same coordination position as the **A** and **B** molecules displayed in red as shown in Figure 2.

The successful encapsulation of **D** into the pores of **2** demonstrates the ability of **2** to potentially encapsulate other non-aromatic thiocarbamate herbicide compounds by taking

advantage of the ability of **2** to form Gd-O coordination bonds with the guest molecules to facilitate guest ordering. This was found to be particularly important when a smaller number of the guest ordering interactions favored by **1** (CH···π and π···π) are able to be formed due to the guests lack of aromaticity.

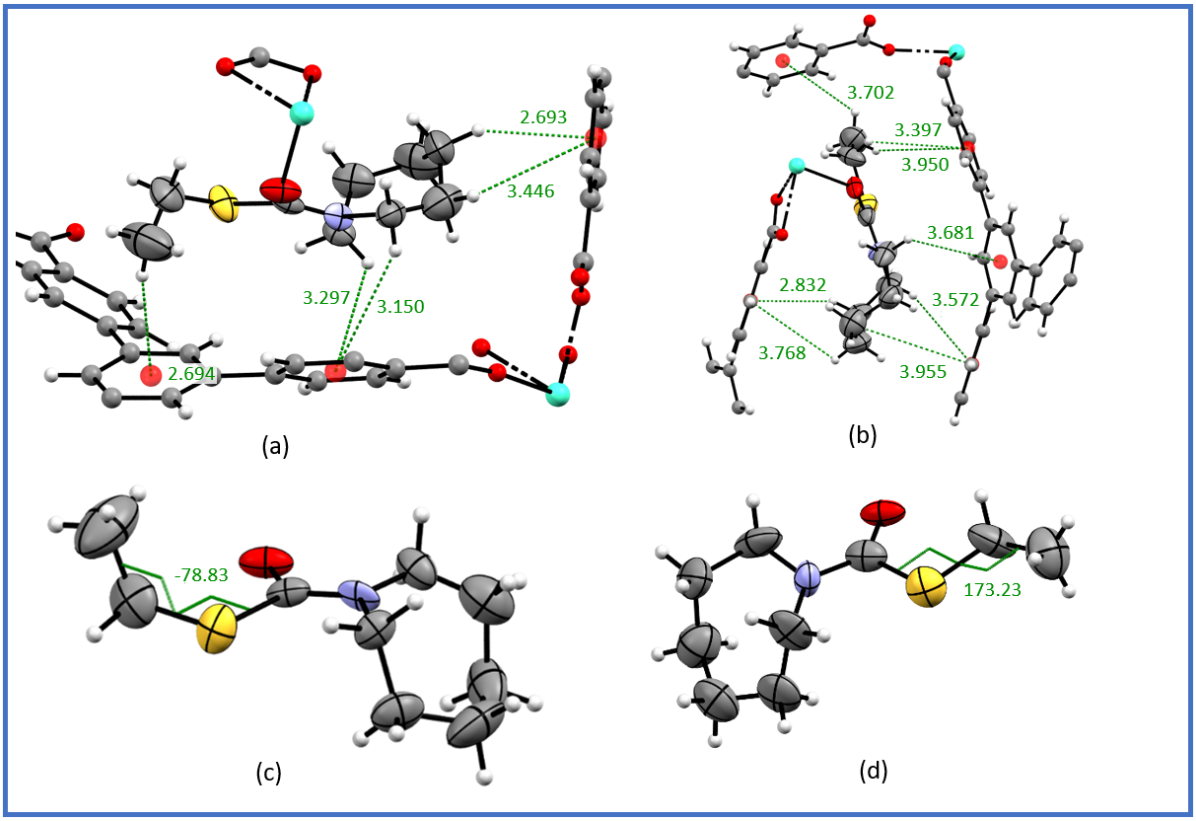

Figure 6. ORTEP diagrams showing guests displayed as ellipsoids at 50% probability and host framework as a ball and stick model. (a) and (b) display the CH-π interactions between the host framework and parts 1 and 2 of the disordered guest molecule respectively. (c) and (d) Illustrations of the torsion angles of part 1 and part 2 respectively. Centroids displayed as red spheres, interactions and torsion angles are represented as green dotted lines. Interaction distances are displayed in angstroms and angles in degrees.

Encapsulation of Vanillin

The encapsulation procedure was changed to encapsulate **E** as it is a powder. As methanol was already encapsulated within the pores of **2** it was thought to be the ideal solvent to dissolve vanillin and facilitate its encapsulation.

Similarly to guest **C** and carvone (as reported by de Gelder *et al*.[26]), when encapsulated into the host, **E** does not coordinate with the MOF metal centre; again this is most likely due to steric constraints. One molecule of **E** was found in the asymmetric unit, this molecule sits in a position within the MOF pores that is different to the aforementioned guests. In a similar manner to both guest molecules of **C**, **E** is disordered over two positions due to inversion symmetry. Interestingly in this case the two disordered components have one carbon atom in common (C34). This atom is found in two different positions within the structure of vanillin: the aldehyde group and the aryloxy group as illustrated in Figure 7. Four guest molecules of **E** have previously been encapsulated into the asymmetric unit of **1** as reported by Ramadhar *et al*.. In contrast to the encapsulation into **2**, the space group symmetry of **1** was reduced from $C2/c$ to $P\overline{1}$ and none of the guest molecules sit on centres of inversion.[19]

The guest was located between two BTB linkers and their metal centres which have two solvent molecules coordinated (one methanol and one water). Therefore, if hydrogen atoms are added to carbons C29, C30, C32 and C33 of the vanillin guest model then it is apparent that **E** was ordered within the MOF pores via a series of π···π and CH···π intermolecular interactions between the guest and the BTB linkers either side of the guests aromatic plane. Hydrogen bonding interactions also form between the guest molecule and host framework; one hydrogen bond forms between the hydroxyl group of the guest and a carboxylate oxygen of the BTB linker. The other hydrogen bonds are formed between the water molecule and methanol molecule, which are coordinated with the gadolinium metal of the host framework either side of the guest molecule, and the hydroxyl, aldehyde and aryloxy groups on the molecule of **E**. Comparatively, when encapsulated within the pores of **1,** π···π and CH···π interactions are also formed between the host framework and guest molecules. Hydrogen bonds are not formed between the guest and the host **1**, however guest - guest hydrogen bonds are formed between the hydroxyl group of one molecule and the aldehyde group of another.[19]

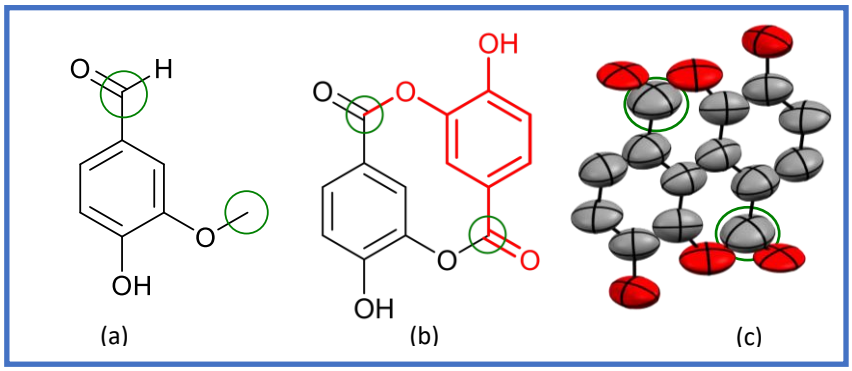

Figure 7. (a) A structure diagram of the vanillin molecule, (b) a structure diagram showing the disorder found in the inclusion complex **2.E** in red and the carbons that overlap within green circles and (c) an ORTEP image showing 50% probability illustrating the carbon atoms that overlap (corresponding to C34 in the crystal structure) in guest **E** within green circles.

Conclusion

The Crystalline sponge method has been successfully employed to encapsulate five guest molecules into the pores of the MOF RUM-2 (2). This includes the first commercial herbicide active ingredient to be encapsulated into a crystalline sponge demonstrating the potential of 2 to encapsulate other non-aromatic thiocarbamate herbicide compounds. The range of chemical structures encountered in herbicide research is diverse.[30] As a result, careful selection of the crystalline sponge material and optimization of soaking conditions will be required for the successful application of the CSM to any specific molecule. Nevertheless, by successfully demonstrating an increased range of options, particularly for compounds only soluble in more polar solvents, the potential of the method in this field has been established. The CSM can now be considered as an option when undertaking the structure elucidation of any otherwise hard to crystallise compounds encountered during the development of new products.

It was observed that three of the guest compounds (**A**, **B** and **D**) can coordinate with the metal atom of the host framework which aids with ordering the guest and substantially increases guest occupancy. As might be expected, there seems to be a limit to the size of guests that can

coordinate with the MOF as guests **C** and **E** do not coordinate despite containing appropriate functional groups. All guest molecules ordered within the MOF pores display a mixture of CH···π and π···π interactions except for the herbicide **D** which could not form π···π interactions due to its lack of aromaticity but was still ordered through guest coordination to the framework and CH···π interactions. All the intermolecular interactions reported here show consistency with interactions reported previously when using the CSM with **1**.[9,19,21,31–33] Most of the guest molecules reported here were found in different locations in the unit cell, though some similarities were noticed such as the guest coordination sites. All guest compounds except **D** have at least one molecule occupying the same site as either a centre of inversion or a two-fold rotation axis. It was also observed that guests can vary their conformation to increase the number of host-guest interactions as was observed in the disordered model of **D**.

Experimental Section

Synthesis of **2** and General Procedure for Guest Inclusion

The synthesis of **2** was performed following a procedure from the literature.[26] After the crystals were synthesised the pore solvent was exchanged with methanol. Crystals were placed into a 14 mL screw capped vial and stored in 10 mL of methanol at 25 °C for a minimum of 4 days until required for guest encapsulation.

A small number of crystals were removed from the storage vial and placed into a new 14 ml screw capped vial. The methanol storage solvent was carefully removed using a glass pipette immediately followed by the addition of 1 ml of neat guest or guest solution into the vial submerging the MOF crystals. The vial was then sealed and placed in an incubator at 25 °C for a period of time (supporting information Table S1) before good quality crystals were chosen for SCXRD analysis.

Crystallographic Method

Crystals were pipetted from the guest solution onto a glass microscope slide. Fomblin oil was used to coat the crystals to prevent them from drying out while a crystal of appropriate quality for single crystal analysis was selected. The selected crystal was mounted onto a nylon loop and transferred to the instrument when it was held in a cryojet stream. An Agilent Super Nova Dual Diffractometer (Agilent Technologies Inc, Santa Clara CA) equipped with Mo – K α radiation (λ = 0.71073 Å) was used to perform the X-ray diffraction analysis at 150 K. The program CrysAlisPro[34] was used to perform unit cell determinations, absorption corrections and data reduction. Structures were solved within the OLEX2 GUI[35] using Direct methods in the Sir2004[36] structure solution program and refined using SHELXL[37] by full matrix least squares on the basis of F^2. Details of the refinement of individual structures, including the modelling of disorder and assigning of guest occupancies are contained in the supplementary material.

Associated Content

Supporting information

The Supporting Information is available free of charge on the ACS Publications Website at DOI:

Crystal data and refinement details, Spacefill unit cell diagrams, encapsulation conditions and experimental considerations. (PDF)

Accession Codes

The CCDC numbers: 1999726, 1999730, 1999738, 1999739, 1999744 contain the supplementary data for this paper. These data can be obtained free of charge via www.ccdc.cam.ac.uk/data_request/cif, or by emailing data_request@ccdc.cam.ac.uk, or by

contacting The Cambridge Crystallographic Data Centre, 12 Union Road, Cambridge CB2 1EZ, UK; fax: +44 1223 336033.

Author Information

Corresponding author:

*Email: c.j.carmalt@ucl.ac.uk. TEL: +44 (0)207 679 7528

Acknowledgments

The EPSRC iCASE award (EP/R512138/1) and Syngenta Ltd are thanked for funding. The authors would also like to acknowledge Dr Jeremy Cockcroft for his crystallographic advice.

Conflicts of interest

The authors declare no conflicts of interest.

References

(1) Inokuma, Y.; Yoshioka, S.; Ariyoshi, J.; Arai, T.; Hitora, Y.; Takada, K.; Matsunaga, S.; Rissanen, K.; Fujita, M. X-Ray Analysis on the Nanogram to Microgram Scale Using Porous Complexes. *Nature* **2013**, *495*, 461–466.

(2) Inokuma, Y.; Yoshioka, S.; Ariyoshi, J.; Arai, T.; Hitora, Y.; Takada, K.; Matsunaga, S.; Rissanen, K.; Fujita, M. Erratum: X-Ray Analysis on the Nanogram to Microgram Scale Using Porous Complexes. *Nature* **2013**, *501*, 262.

(3) Sakurai, F.; Khutia, A.; Kikuchi, T.; Fujita, M. X-Ray Structure Analysis of N-Containing Nucleophilic Compounds by the Crystalline Sponge Method. *Chem. - A Eur. J.* **2017**, *23*, 15035–15040.

(4) Urban, S.; Brkljača, R.; Hoshino, M.; Lee, S.; Fujita, M. Determination of the

Absolute Configuration of the Pseudo-Symmetric Natural Product Elatenyne by the Crystalline Sponge Method. *Angew. Chemie - Int. Ed.* **2016**, *55*, 2678–2682.

(5) Naoki, W.; D., K. R.; Takahiro, I.; Shoukou, L.; Fumie, S.; Takashi, K.; Daishi, F.; Makoto, F.; Jing-Ke, W. Crystalline-Sponge-Based Structural Analysis of Crude Natural Product Extracts. *Angew. Chemie Int. Ed.* **2018**, *57*, 3671–3675.

(6) Inokuma, Y.; Ukegawa, T.; Hoshino, M.; Fujita, M. Structure Determination of Microbial Metabolites by the Crystalline Sponge Method. *Chem. Sci.* **2016**, *7*, 3910–3913.

(7) Mitsuhashi, T.; Kikuchi, T.; Hoshino, S.; Ozeki, M.; Awakawa, T.; Shi, S. P.; Fujita, M.; Abe, I. Crystalline Sponge Method Enabled the Investigation of a Prenyltransferase-Terpene Synthase Chimeric Enzyme, Whose Product Exhibits Broadened NMR Signals. *Org. Lett.* **2018**, *20*, 5606–5609.

(8) Yoshioka, S.; Inokuma, Y.; Duplan, V.; Dubey, R.; Fujita, M. X-Ray Structure Analysis of Ozonides by the Crystalline Sponge Method. *J. Am. Chem. Soc.* **2016**, *138*, 10140–10142.

(9) Gu, X. F.; Zhao, Y.; Li, K.; Su, M. X.; Yan, F.; Li, B.; Du, Y. X.; Di, B. Differentiation of Volatile Aromatic Isomers and Structural Elucidation of Volatile Compounds in Essential Oils by Combination of HPLC Separation and Crystalline Sponge Method. *J. Chromatogr. A* **2016**, *1474*, 130–137.

(10) Ikemoto, K.; Inokuma, Y.; Rissanen, K.; Fujita, M. X-Ray Snapshot Observation of Palladium-Mediated Aromatic Bromination in a Porous Complex. *J. Am. Chem. Soc.* **2014**, *136*, 6892–6895.

(11) Du, Q.; Peng, J.; Wu, P.; He, H. Review: Metal-Organic Framework Based Crystalline

Sponge Method for Structure Analysis. *TrAC - Trends Anal. Chem.* **2018**, *102*, 290–310.

(12) Kawamichi, T.; Haneda, T.; Kawano, M.; Fujita, M. X-Ray Observation of a Transient Hemiaminal Trapped in a Porous Network. *Nature* **2009**, *461*, 633–635.

(13) Vincent, D.; Manabu, H.; Wei, L.; Tadashi, H.; Makoto, F. In Situ Observation of Thiol Michael Addition to a Reversible Covalent Drug in a Crystalline Sponge. *Angew. Chemie - Int. Ed.* **2016**, *55*, 4919–4923.

(14) Cuenca, A. B.; Zigon, N.; Duplan, V.; Hoshino, M.; Fujita, M.; Fernández, E. Undeniable Confirmation of the Syn-Addition Mechanism for Metal-Free Diboration by Using the Crystalline Sponge Method. *Chem. - A Eur. J.* **2016**, *22*, 4723–4726.

(15) Biradha, K.; Fujita, M. A Springlike 3D-Coordination Network That Shrinks or Swells in a Crystal-to-Crystal Manner upon Guest Removal or Readsorption. *Angew. Chemie - Int. Ed.* **2002**, *41*, 3392–3395.

(16) Ramadhar, T. R.; Zheng, S. L.; Chen, Y. S.; Clardy, J. Analysis of Rapidly Synthesized Guest-Filled Porous Complexes with Synchrotron Radiation: Practical Guidelines for the Crystalline Sponge Method. *Acta Crystallogr. Sect. A Found. Crystallogr.* **2015**, *71*, 46–58.

(17) Hoshino, M.; Khutia, A.; Xing, H.; Inokuma, Y.; Fujita, M. The Crystalline Sponge Method Updated. *IUCrJ* **2016**, *3*, 139–151.

(18) Waldhart, G. W.; Mankad, N. P.; Santarsiero, B. D. Improvements to the Practical Usability of the “Crystalline Sponge” Method for Organic Structure Determination. *Org. Lett.* **2016**, *18*, 6112–6115.

(19) Ramadhar, T. R.; Zheng, S. L.; Chen, Y. S.; Clardy, J. The Crystalline Sponge Method: A Solvent-Based Strategy to Facilitate Noncovalent Ordered Trapping of Solid and Liquid Organic Compounds. *CrystEngComm* **2017**, *19*, 4528–4534.

(20) Inokuma, Y.; Matsumura, K.; Yoshioka, S.; Fujita, M. Finding a New Crystalline Sponge from a Crystallographic Database. *Chem. - An Asian J.* **2017**, *12*, 208–211.

(21) Hayes, L. M.; Knapp, C. E.; Nathoo, K. Y.; Press, N. J.; Tocher, D. A.; Carmalt, C. J. The Crystalline Sponge Method: A Systematic Study of the Reproducibility of Simple Aromatic Molecule Encapsulation and Guest-Host Interactions. *Cryst. Growth Des.* **2016**, *16*, 3465–3472.

(22) Ning, G. H.; Matsumura, K.; Inokuma, Y.; Fujita, M. A Saccharide-Based Crystalline Sponge for Hydrophilic Guests. *Chem. Commun.* **2016**, *52*, 7013–7015.

(23) Qin, J. S.; Yuan, S.; Alsalme, A.; Zhou, H. C. Flexible Zirconium MOF as the Crystalline Sponge for Coordinative Alignment of Dicarboxylates. *ACS Appl. Mater. Interfaces* **2017**, *9*, 33408–33412.

(24) Lee, S.; Kapustin, E. A.; Yaghi, O. M. Coordinative Alignment of Molecules in Chiral Metal-Organic Frameworks. *Science!* **2016**, *353*, 808–811.

(25) Wang, L.; Moore, C. E.; Cohen, S. M. Coordinative Alignment to Achieve Ordered Guest Molecules in a Versatile Molecular Crystalline Sponge. *Cryst. Growth Des.* **2017**, *17*, 6174–6177.

(26) de Poel, W.; Tinnemans, P.; Duchateau, A. L. L.; Honing, M.; Rutjes, F. P. J. T.; Vlieg, E.; de Gelder, R. The Crystalline Sponge Method in Water. *Chem. - A Eur. J.* **2019**, *25*, 14999–15003.

(27) Oelke, E. A.; Morse, M. D. Propanil and Molinate for Control of Barnyardgrass in Water-Seeded Rice. *Weed Sci.* **1968**, *16*, 235–239.

(28) HRAC_Revised_MOA_Classification_Herbicides_Poster.png https://hracglobal.com/files/HRAC_Revised_MOA_Classification_Herbicides_Poster.png (accessed Sep 7, 2020).

(29) Macrae, C. F.; Bruno, I. J.; Chisholm, J. A.; Edgington, P. R.; McCabe, P.; Pidcock, E.; Rodriguez-Monge, L.; Taylor, R.; Van De Streek, J.; Wood, P. A. Mercury CSD 2.0 - New Features for the Visualization and Investigation of Crystal Structures. *J. Appl. Crystallogr.* **2008**, *41*, 466–470.

(30) Still, G. G.; Davis, D. G.; Zander, G. L. Plant Epicuticular Lipids: Alteration by Herbicidal Carbamates. *Plant Physiol.* **1970**, *46*, 307–314.

(31) Brunet, G.; Safin, D. A.; Robeyns, K.; Facey, G. A.; Korobkov, I.; Filinchuk, Y.; Murugesu, M. Confinement Effects of a Crystalline Sponge on Ferrocene and Ferrocene Carboxaldehyde. *Chem. Commun.* **2017**, *53*, 5645–5648.

(32) Li, K.; Yang, D. S.; Gu, X. F.; Di, B. Absolute Configuration Determination of Asarinin by Synchrotron Radiation with Crystalline Sponge Method. *Fitoterapia* **2019**, *134*, 135–140.

(33) Hayes, L. M.; Press, N. J.; Tocher, D. A.; Carmalt, C. J. Intermolecular Interactions between Encapsulated Aromatic Compounds and the Host Framework of a Crystalline Sponge. *Cryst. Growth Des.* **2017**, *17*, 858–863.

(34) CrysAlisPRO. Agilent Technologies Ltd: Yarnton, Oxfordshire, England 2014.

(35) Dolomanov, O. V; Bourhis, L. J.; Gildea, R. J.; Howard, J. A. K.; Puschmann, H.

OLEX2: A Complete Structure Solution, Refinement and Analysis Program. *J. Appl. Crystallogr.* **2009**, *42*, 339–341.

(36) Burla, M. C.; Caliandro, R.; Camalli, M.; Carrozzini, B.; Cascarano, G. L.; De Caro, L.; Giacovazzo, C.; Polidori, G.; Spagna, R. SIR2004: An Improved Tool for Crystal Structure Determination and Refinement. *J. Appl. Crystallogr.* **2005**, *38*, 381–388.

(37) Sheldrick, G. M. Crystal Structure Refinement with SHELXL. *Acta Crystallogr. Sect. C* **2015**, *71*, 3–8.

For Table of Contents Use Only

Encapsulation of Aromatic Compounds and a Non-Aromatic Herbicide into a Gadolinium Based Metal-Organic Framework via the Crystalline Sponge Method

Richard D. J. Lunn,[†] Derek A. Tocher,[†] Philip J. Sidebottom,[‡] Mark G. Montgomery,[‡] Adam C. Keates,[‡] Claire J. Carmalt[*†]

[†]UCL Department of Chemistry, 20 Gordon Street, London, WC1H 0AJ

[‡]Syngenta, Jealott's Hill International Research Centre, Bracknell, Berkshire, RG42 6EY

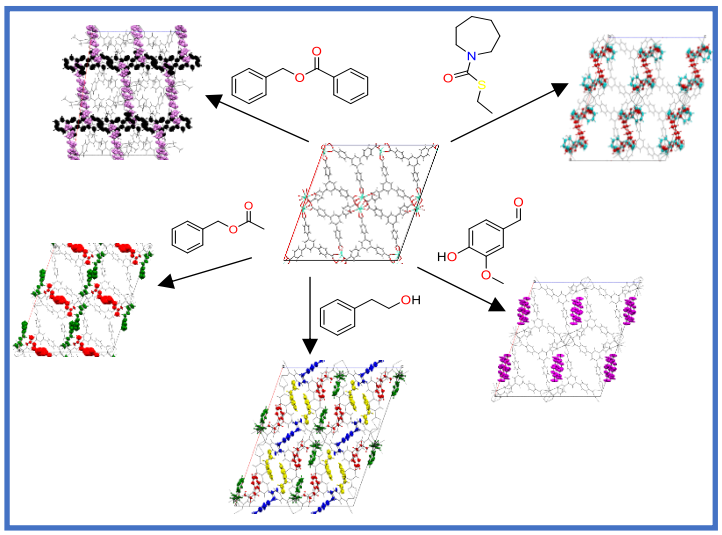

Here we report five novel inclusion complexes within the crystalline sponge RUM-2 including the first commercial herbicide to have its structure elucidated by the crystalline sponge method, molinate. A detailed investigation was performed into the effect of guest size on the position the guests sit within the MOF pores and the different intermolecular interactions used for guest ordering.